

# Exploring the small mass ratio binary black hole merger via Zeno's dichotomy approach\*

Carlos O. Lousto and James Healy

*Center for Computational Relativity and Gravitation,  
School of Mathematical Sciences, Rochester Institute of Technology,  
85 Lomb Memorial Drive, Rochester, New York 14623*

(Dated: April 24, 2022)

We perform a sequence of binary black hole simulations with increasingly small mass ratios, reaching a 128:1 binary that displays 13 orbits before merger. Based on a detailed convergence study of the  $q = m_1/m_2 = 1/15$  nonspinning case, we apply additional mesh refinements levels on the smaller hole horizon to reach the  $q = 1/32$ ,  $q = 1/64$ , and  $q = 1/128$  cases. Roughly linear strong computational scaling with  $1/q$  is observed on 8-nodes simulations. We compute the remnant properties of the merger; final mass, spin, and recoil velocity. We also compute the gravitational waveforms, peak frequency, amplitude, and luminosity. We compare those values with predictions of the corresponding phenomenological formulas, reproducing the particle limit, and we then use these new results to improve their fitting coefficients.

## INTRODUCTION

While ground based gravitational wave detectors like LIGO [1] are particularly sensitive to comparable (stellar) mass binaries, third generation ground detectors [2] and space detectors, like LISA, will also be sensitive to the observation of very unequal mass binary black holes [3]. The evolution of these small mass ratio binaries have been approached via perturbations theory and the computation of the gravitational self-force exerted by the field of the small black hole on itself [4]. The resolution of the binary black hole problem in its full nonlinearity have been only possible after the breakthroughs in numerical relativity [5–7], and a first proof of principle have been performed in [8] for the 100:1 mass ratio case, following studies of 10:1 and 15:1 [9]. In the particular case of [8] the evolution covered two orbits before merger, and while this proved that evolutions are possible, practical application of their gravitational waveforms requires longer evolutions. Here we report on a new set of evolutions that are based on the numerical techniques [10] refined for the longterm evolution of a spinning precessing binary with mass ratio  $q = m_1/m_2 = 1/15$ . The case of nonspinning  $q = 1/15$  is here studied in a convergence sequence to assess numerical and systematical errors and we add a sequence of  $q = 1/32$ ,  $q = 1/64$ ,  $q = 1/128$ , nonspinning binaries evolutions for a dozen orbits before merger.

## SIMULATION'S RESULTS

For the  $q = 1/15$  case, we performed three globally increasing resolution simulations (labeled by its number of points per total mass  $m$ , n100, n120, n140, at the waveform extraction zone, about  $100 - 150m$  away from the binary). The simulations start at a coordinate separation  $D = 10m$ , or about a simple proper horizon distance

(along the coordinate line joining the holes),  $SPD=12m$ . The inspiral evolution follows for about 19 orbits (about  $t = 3240m$ ) before merger and forms a final black hole with the characteristics summarized in Table I. The n100 simulation proceeded at a speed of  $2.7m/hr$  on 8 TACC's (<https://www.tacc.utexas.edu>) stampede2 nodes, totaling a 10,540 node hours run.

The high convergence of these results allow us to use the lowest of the resolutions, n100, to perform a set of smaller  $q$  simulations by each time halving the mass ratio. In order to maintain the accuracy at this base resolution and account for the longer merger time scale we reduce the initial distance (and hence the evolution time) as shown in Table II. Where we also display the final black hole remnant and peak waveform properties.

Figure 1 makes a comparative display of the four  $q$  waveforms, (2,2)-modes of the strain, in the same scale to show the differences in merger amplitude and evolution time. While Fig. 2 displays the comparative merger time from a fiducial initial orbital frequency  $m\Omega_i = 0.0465$  (corresponding roughly to coordinate separation  $D = 7m$  and simple proper distance  $SPD = 8.5m$ ) to merger for the mass ratios  $q = 1/15, 1/32, 1/64, 1/128$  simulations. We observe a time to merger  $t_m \sim (83.2 \pm 8.5)m\eta^{-0.56 \pm 0.03}$  dependence for small mass ratios, and interpret it as a composed power of the leading rates from the post-Newtonian regime [11]:  $q^{-1}$  from the inspiral decay and  $q^0$  from the plunge.

The simulations of  $q = 1/32, 1/64, 1/128$  use an 8th order stencil in space [12] and 4th order in time (with  $dt = dx/4$ ) and have all been performed in TACC's Frontera cluster on 8 nodes at speeds 1.1, 0.6, and 0.32  $m$  per hour totaling 13,807, 17,713, and 41,250 node hours respectively. Thus showing a notable approximately linear scaling with inverse of the mass ratio.

TABLE I. The final black hole mass  $M_{\text{rem}}/m$ , spin  $\alpha_{\text{rem}}$ , and its recoil velocity  $v_m$ , and the Luminosity  $\mathcal{L}$ , waveform frequency  $\omega_{22}$  at the maximum amplitude  $h_{\text{peak}}$ , for each resolution of the  $q = 1/15$  simulations. Extrapolation to infinite resolution and order of convergence is derived.

resolution	$M_{\text{rem}}/m$	$\alpha_{\text{rem}}$	$v_m$ [km/s]	$\mathcal{L}_{\text{peak}}$ [ergs/s]	$m\omega_{22}^{\text{peak}}$	$h_{\text{peak}}$
n100	0.994837	0.188442	33.45	1.659e+55	0.2902	0.08526
n120	0.994876	0.188874	34.67	1.678e+55	0.2860	0.08473
n140	0.994891	0.188987	35.24	1.683e+55	0.2866	0.08466
$n \rightarrow \infty$	0.994905	0.189047	36.07	1.687e+55	0.2868	0.08464
order	4.63	6.87	3.40	6.01	10.33	10.82

TABLE II. The final black hole mass  $M_{\text{rem}}/m$ , spin  $\alpha_{\text{rem}}$ , and its recoil velocity  $v_m$ , and the Luminosity  $\mathcal{L}$ , waveform frequency  $\omega_{22}$  at the maximum amplitude  $h_{\text{peak}}$ , for the sequence of the  $q = 1/32, 1/64, 1/128$  simulations. Also given are the initial simple proper distance, SPD, and number of orbits to merger  $N$  for these simulations.

$q$	$M_{\text{rem}}/m$	$\alpha_{\text{rem}}$	$v_m$ [km/s]	$\mathcal{L}_{\text{peak}}$ [ergs/s]	$m\omega_{22}^{\text{peak}}$	$h_{\text{peak}}$	SPD	N
1/32	0.9979	0.1006	9.14	4.260e+54	0.2820	0.0424	9.51	13.02
1/64	0.9990	0.0520	2.34	1.113e+54	0.2812	0.0220	8.22	9.98
1/128	0.9996	0.0239	0.96	3.313e+53	0.2746	0.0116	8.19	12.90

## COMPARISONS VS. PREDICTIONS

An important test of the accuracy of our simulations is to compare the final properties in Table II versus the predictions of the formulas obtained in Ref. [13] for them. We display these results in Fig. 3. We stress that in this figure there is no fitting being performed to the new data, but a raw comparison of the previous formulas extrapolated to a previously uncovered region of small  $q$ .

In the light of these good results, we can now use the current data to generate a new fit of the nonspinning binary remnant and merger waveform properties. We will also correct for the center of mass motion[14], of particular relevance for comparable masses, in these new fits, which was not included for all quantities in Ref. [13]. In practice, the center of mass motion for these nonspinning systems is small, and primarily only affects the recoil velocity. We find that after correction, the recoil velocities change by at most 2%, well within the error from finite resolution (5-10%).

For the unequal mass expansion of the final mass and spin of the merged black holes we will use the forms from [15] that include the particle limit. The fitting formula for  $M_{\text{rem}}$  is given by,

$$\frac{M_{\text{rem}}}{m} = (4\eta)^2 \left\{ M_0 + K_{2d} \delta m^2 + K_{4f} \delta m^4 \right\} + \left[ 1 + \eta(\tilde{E}_{\text{ISCO}} + 11) \right] \delta m^6, \quad (1)$$

where  $\delta m = (m_1 - m_2)/m$  and  $m = (m_1 + m_2)$  and  $4\eta = 1 - \delta m^2$ .

And the fitting formula for the final spin has the form,

$$\alpha_{\text{rem}} = \frac{S_{\text{rem}}}{M_{\text{rem}}^2} = (4\eta)^2 \left\{ L_0 + L_{2d} \delta m^2 + L_{4f} \delta m^4 \right\} + \eta \tilde{J}_{\text{ISCO}} \delta m^6. \quad (2)$$

Note that the two formulae above impose the particle limit by including the ISCO dependencies,  $\tilde{E}_{\text{ISCO}}(\alpha_{\text{rem}})$ , and  $\tilde{J}_{\text{ISCO}}(\alpha_{\text{rem}})$  (See Ref. [15, 16] for the explicit expressions).

For the nonspinning recoil we will use Ref. [13] parametrization

$$v_m = \eta^2 \delta m (A + B \delta m^2 + C \delta m^4). \quad (3)$$

We model the peak amplitude (of the strain  $h$ ) from the merger of nonspinning binaries using the expansion [17]

$$h_{\text{peak}} = (4\eta)^2 \left\{ H_0 + H_{2d} \delta m^2 + H_{4f} \delta m^4 \right\} + \eta \tilde{H}_p \delta m^6, \quad (4)$$

where  $\tilde{H}_p(\alpha_{\text{rem}})$  is the particle limit, taking the value  $H_p(0) = 1.4552857$  in the nonspinning limit [18].

The formula to model the peak luminosity introduced in [17] takes the following simple form for nonspinning binaries

$$\mathcal{L}_{\text{peak}} = (4\eta)^2 \left\{ N_0 + N_{2d} \delta m^2 + N_{4f} \delta m^4 \right\}. \quad (5)$$

Analogously to the previous formula we model the peak frequency of the (2,2) mode of the gravitational wave strain for nonspinning binaries

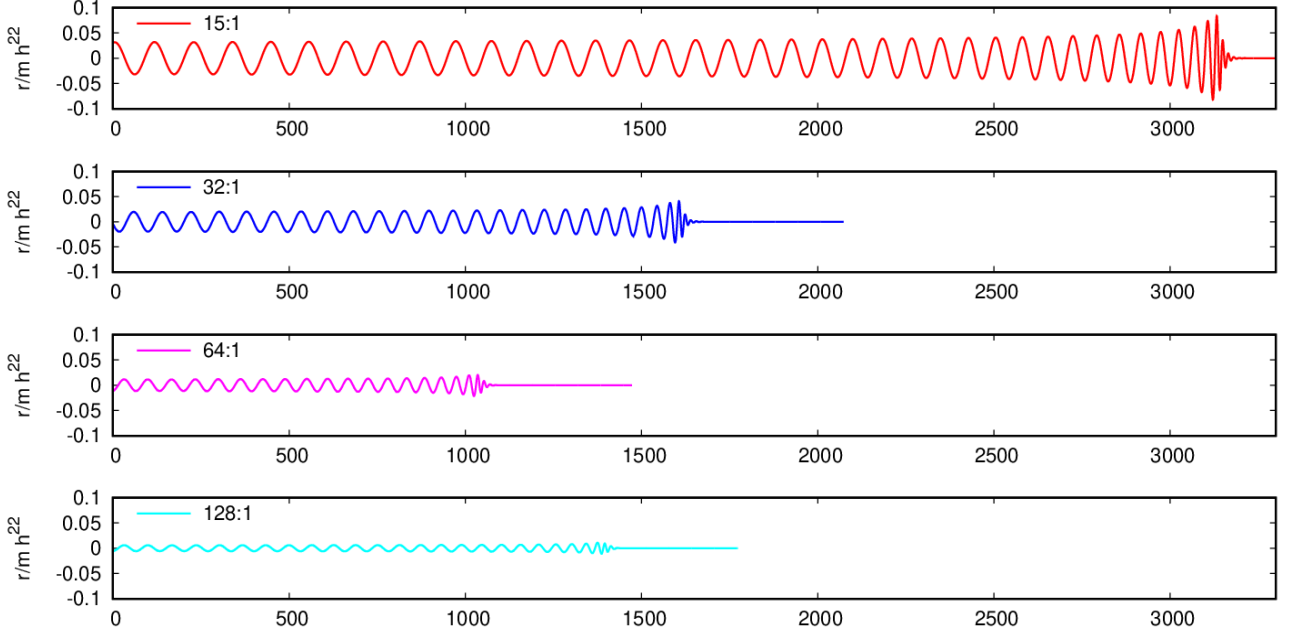


FIG. 1. (2,2) modes (real part) of the strain waveforms versus time ( $t/m$ ), for the  $q = 1/15, 1/32, 1/64, 1/128$  simulations.

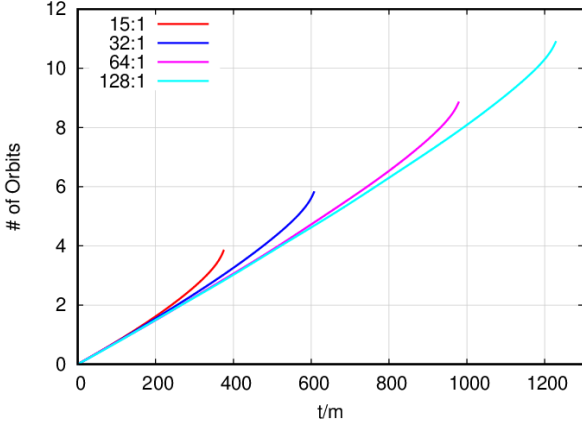


FIG. 2. Comparative number of orbits and time to merger, from a fiducial orbital frequency  $m\Omega_i = 0.0465$  for the  $q = 1/15, 1/32, 1/64, 1/128$  simulations.

TABLE III. Fitting coefficients of the phenomenological formulas (1)-(6)

$M_0$	$K_{2d}$	$K_{4f}$
$0.95165 \pm 0.00002$	$1.99604 \pm 0.00029$	$2.97993 \pm 0.00066$
$L_0$	$L_{2d}$	$L_{4f}$
$0.68692 \pm 0.00065$	$0.79638 \pm 0.01086$	$0.96823 \pm 0.02473$
$A$	$B$	$C$
$-8803.17 \pm 104.60$	$-5045.58 \pm 816.10$	$1752.17 \pm 1329.00$
$N_0 \times 10^3$	$N_{2d} \times 10^4$	$N_{4f} \times 10^4$
$(1.0213 \pm 0.0004)$	$(-4.1368 \pm 0.0652)$	$(2.46408 \pm 0.1485)$
$W_0$	$W_{2d}$	$W_{4f}$
$0.35737 \pm 0.00097$	$0.26529 \pm 0.01096$	$0.22752 \pm 0.01914$
$H_0$	$H_{2d}$	$H_{4f}$
$0.39357 \pm 0.00015$	$0.34439 \pm 0.00256$	$0.33782 \pm 0.00584$

## CONCLUSIONS

This study represents a new milestone for comparative studies of improvements in the code efficiency and on gauge and initial data improvements, and it allows to begin massive production of small mass ratio simulations to populate the next release of the RIT catalog of binary black hole waveforms (<https://ccrg.rit.edu/~RITCatalog>). In particular, the simulation of mass ratio 128:1 presented here is a record breaking numerical relativity run and it includes nearly 13 orbits before merger. The particle limit remnant and peak waveform parameters are reproduced within 1-2% errors with

$$m\omega_{22}^{\text{peak}} = (4\eta) \left\{ W_0 + W_{2d} \delta m^2 + W_{4f} \delta m^4 \right\} + \tilde{\Omega}_p \delta m^6, \quad (6)$$

where  $\tilde{\Omega}_p(\alpha_{\text{rem}})$  is the particle limit, taking the value  $\tilde{\Omega}_p(0) = 0.279525$  in the nonspinning limit [18].

Table III summarizes the new values of all those coefficients with their estimated errors.

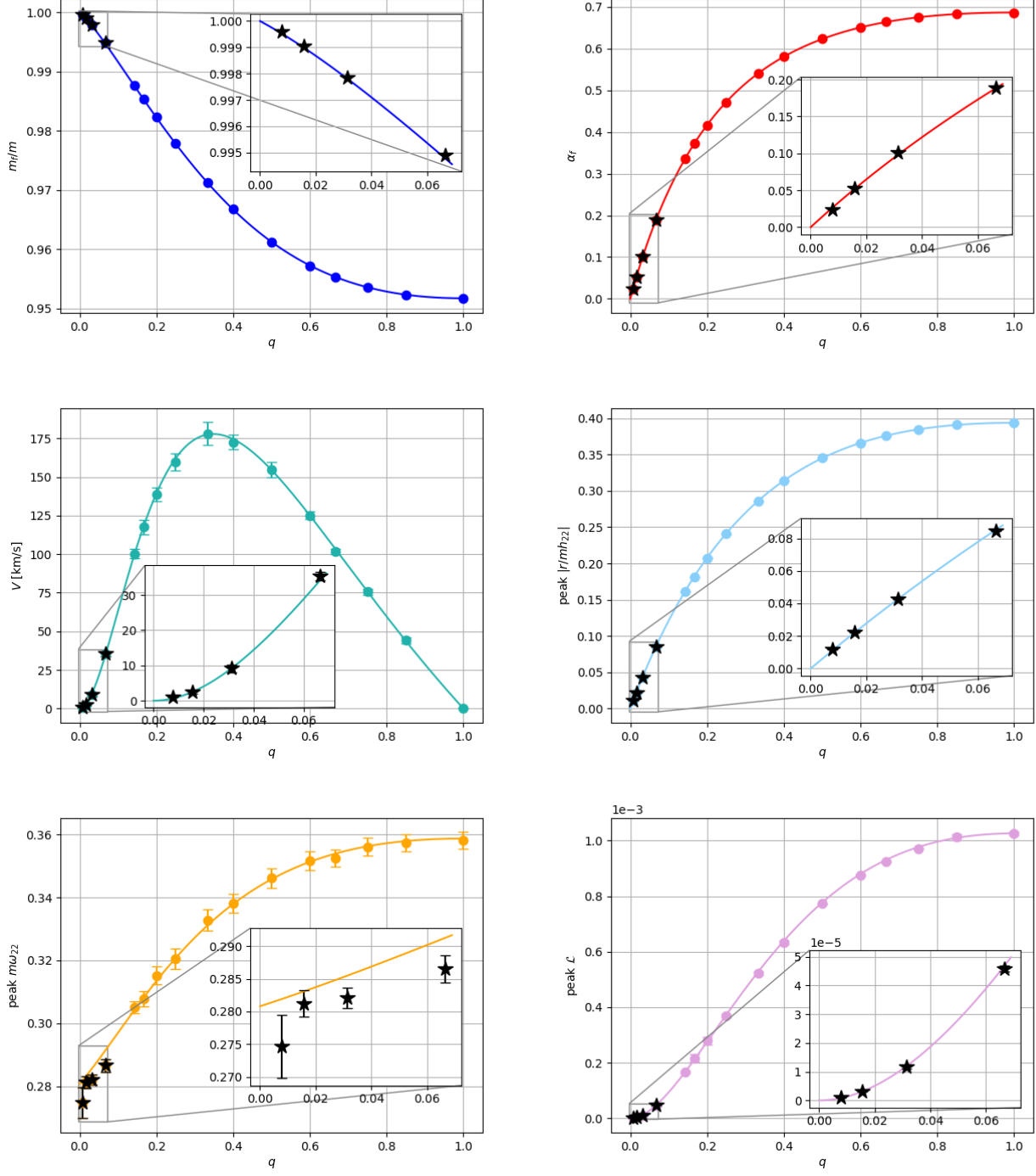


FIG. 3. Final mass, spin, recoil velocity, peak amplitude, frequency, and luminosity. Predicted vs. current results for the  $q = 1/15, 1/32, 1/64, 1/128$  simulations. Each panel contains the prediction from the original fits in Ref. [13] (solid line), data used to determine the original fits (filled circles), and the data for the current results (stars). An inset in each panel zooms in on the new simulations. Again, we stress no fitting to the new data is performed in this plot.

purely full numerical methods. The extension to include (high) spins into the large black hole seems straightforward with our current techniques[19]. Those simulations can be used in both, direct observations by advanced,

3rd generation ground based gravitational wave detectors and for the space project LISA.

The authors also gratefully acknowledge the National Science Foundation (NSF) for financial support from

Grants No. PHY-1912632 and PHY-1238993. This work used the Extreme Science and Engineering Discovery Environment (XSEDE) [allocation TG-PHY060027N], which is supported by NSF grant No. ACI-1548562. Computational resources were also provided by the NewHorizons, BlueSky Clusters, and Green Prairies at the Rochester Institute of Technology, which were supported by NSF grants No. PHY-0722703, No. DMS-0820923, No. AST-1028087, No. PHY-1229173, and No. PHY-1726215. Computational resources were also provided by Frontera projects PHY-20010 and PHY-20007. Frontera is an NSF-funded petascale computing system at the Texas Advanced Computing Center (TACC).

---

\* The title refers to our approach of halving and halving the mass ratio while adding internal grid refinement levels to the well studied  $q = 1/15$  case, inspired by the first of Zeno's paradoxes, as reported by Aristotle [20]. J.L.Borges [21], in *Death and the Compass*, writes "I know of a Greek labyrinth which is a single straight line. Along this line so many philosophers have lost themselves..."

- [1] B. P. Abbott *et al.* (LIGO Scientific, Virgo), Phys. Rev. **D100**, 104036 (2019), arXiv:1903.04467 [gr-qc].
- [2] M. Pürrer and C.-J. Haster, Phys. Rev. Res. **2**, 023151 (2020), arXiv:1912.10055 [gr-qc].
- [3] J. R. Gair, S. Babak, A. Sesana, P. Amaro-Seoane, E. Barausse, C. P. Berry, E. Berti, and C. Sopuerta, J. Phys. Conf. Ser. **840**, 012021 (2017), arXiv:1704.00009 [astro-ph.GA].
- [4] L. Barack and A. Pound, Rept. Prog. Phys. **82**, 016904 (2019), arXiv:1805.10385 [gr-qc].
- [5] F. Pretorius, Phys. Rev. Lett. **95**, 121101 (2005), gr-qc/0507014.
- [6] M. Campanelli, C. O. Lousto, P. Marronetti, and Y. Zlochower, Phys. Rev. Lett. **96**, 111101 (2006), gr-qc/0511048.
- [7] J. G. Baker, J. Centrella, D.-I. Choi, M. Koppitz, and J. van Meter, Phys. Rev. Lett. **96**, 111102 (2006), gr-qc/0511103.
- [8] C. O. Lousto and Y. Zlochower, Phys. Rev. Lett. **106**, 041101 (2011), arXiv:1009.0292 [gr-qc].
- [9] C. O. Lousto, H. Nakano, Y. Zlochower, and M. Campanelli, Phys. Rev. **D82**, 104057 (2010), arXiv:1008.4360 [gr-qc].
- [10] C. O. Lousto and J. Healy, Phys. Rev. Lett. **114**, 141101 (2015), arXiv:1410.3830 [gr-qc].
- [11] L. E. Kidder, C. M. Will, and A. G. Wiseman, Phys. Rev. **D47**, 3281 (1993).
- [12] C. O. Lousto and Y. Zlochower, Phys. Rev. **D77**, 024034 (2008), arXiv:0711.1165 [gr-qc].
- [13] J. Healy, C. O. Lousto, and Y. Zlochower, Phys. Rev. **D96**, 024031 (2017), arXiv:1705.07034 [gr-qc].
- [14] C. J. Woodford, M. Boyle, and H. P. Pfeiffer, Phys. Rev. **D100**, 124010 (2019), arXiv:1904.04842 [gr-qc].
- [15] J. Healy, C. O. Lousto, and Y. Zlochower, Phys. Rev. **D90**, 104004 (2014), arXiv:1406.7295 [gr-qc].
- [16] A. Ori and K. S. Thorne, Phys. Rev. **D62**, 124022 (2000), arXiv:gr-qc/0003032.
- [17] J. Healy and C. O. Lousto, Phys. Rev. **D95**, 024037 (2017), arXiv:1610.09713 [gr-qc].
- [18] A. Bohé *et al.*, Phys. Rev. **D95**, 044028 (2017), arXiv:1611.03703 [gr-qc].
- [19] I. Ruchlin, J. Healy, C. O. Lousto, and Y. Zlochower, Phys. Rev. **D95**, 024033 (2017), arXiv:1410.8607 [gr-qc].
- [20] Aristotle, *Physics*, Vol. VI:9 (350BCE) p. 239b10.
- [21] J. L. Borges, *Collected Fictions* (Penguin Classics Deluxe Edition, London, 1999).